processes

MDPI

Article

Biochemical and Functional Characterization by Site-Directed Mutagenesis of a Phospholipase A_2 from *Scorpio maurus* Venom

Najeh Krayem [1], Mona Alonazi [2], Bassem Khemakhem [3], Habib Horchani [4], Slim Cherif [1], Aida Karray [1] and Abir Ben Bacha [2,*]

[1] Laboratory of Biochemistry and Enzymatic Engineering of Lipases, ENIS, University of Sfax, Soukra Road, BP1171, Sfax 3038, Tunisia; krayemnajeh@yahoo.fr (N.K.); slimcherif_enis@yahoo.fr (S.C.); karrayaida_biotech@yahoo.fr (A.K.)
[2] Department of Biochemistry, College of Science, King Saud University, P.O. Box 22452, Riyadh 11495, Saudi Arabia; moalonazi@ksu.edu.sa
[3] Laboratory of Plant Biotechnology, Sfax Faculty of Sciences, University of Sfax, BP 1171, Sfax 3038, Tunisia; bassem.khemakhem@fss.usf.tn
[4] Science Department, College of Rivière-Du-Loup, Rivière-Du-Loup, QC G5R 1R1, Canada; habib.horchani@cegeprdl.ca
* Correspondence: aalghanouchi@ksu.edu.sa; Tel.: +966-11-8050129

Abstract: The study of amino acid interactions in the active site of scorpion venom phospholipases A_2 could help to gain insights into the structure–function relationship and the biological activities of the enzyme. In the secreted phospholipase A_2 of *Scorpio maurus* venom glands, Glutamate 63 and Tyrosine 122 amino acids play critical roles in the catalytic mechanism through interactions with residues around the calcium-binding loop. We constructed mutants at these positions by overexpression in *Escherichia coli* cells. After refolding and purification of recombinant enzymes, we studied their kinetic properties using pH-stat and monolayer techniques. The mutant Glutamate 63–Aspartate (E63D) exhibited a reduced activity, while the second mutant Tyrosine 122–Arginine (Y122R) retained some activity with a 14-fold reduction in catalytic efficiency. However, both mutants remained stable in pH values ranging from 2 to 12 whereas the double mutant D63–R122 was catalytically inactive. Comparative analysis of wild-type and mutant 3-D models showed various modifications of the hydrogen-binding network linking residues Glutamate 63 and Tyrosine 122. These modifications of interactions could explain the reduction in enzymatic activity. The kinetic behavior on phosphatidylcholine and phosphatidylethanolamine monolayers of three mutants was evaluated using a baro-stat system to assess the potential association between the hydrolysis of erythrocyte membrane phospholipids and the enzyme's capability to penetrate phospholipid monolayers at high surface pressure. Mutants' kinetic behaviors were similar to the wild-type form with slightly modified specific activities at high surface pressure. All mutants were more active on phosphatidylethanolamine than phosphatidylcholine films at high surface pressure. This study provided new information to further elucidate structure–function relationships of scorpion venom-secreted phospholipases A_2 and the design of novel potent drug molecules.

Keywords: secreted phospholipase A_2; *Scorpio maurus*; venom gland; mutant; kinetic property; pH stability

Citation: Krayem, N.; Alonazi, M.; Khemakhem, B.; Horchani, H.; Cherif, S.; Karray, A.; Ben Bacha, A. Biochemical and Functional Characterization by Site-Directed Mutagenesis of a Phospholipase A_2 from *Scorpio maurus* Venom. *Processes* **2023**, *11*, 3364. https://doi.org/10.3390/pr11123364

Academic Editors: Carla Silva and Kwang Yeon Hwang

Received: 6 October 2023
Revised: 12 November 2023
Accepted: 1 December 2023
Published: 4 December 2023

1. Introduction

Secreted phospholipases A_2 ($sPLA_2$s) hydrolyze the n-2 ester bonds of glycerophospholipids. They are widely found in biological liquids such as pancreatic juices and especially in animal venoms like snake, bee, and scorpion. $sPLA_2$s are characterized by small molecular masses between 13 and 15 kDa, containing six to eight disulfide bonds, Histidine (His)/Aspartate (Asp) catalytic residues, and require a millimolar concentration of calcium (Ca^{2+}) for enzymatic activities [1]. According to the amino acid sequence and

similarities, $sPLA_2$ enzymes include 12 groups, namely I (A and B), II (A–F), III, V, X, IX, XII (A and B), and otoconin-95. Groups IA, IIA, IIB, III, and IX are present in venoms [2].

Snake venom $sPLA_2$s are classified into group I and group II based on the presence or absence of a pancreatic loop, C-terminal extension, and disulfide bond number [3]. Despite their structure similitudes, snake venom $sPLA_2$s are characterized by many pharmacological activities such as inflammatory, neurotoxicity, anticoagulant, anti-tumoral, and anti-microbial properties [3]. Group III $sPLA_2$ has been found in the venom of bees, lizards, jellyfish, bumblebees, and scorpions [4]. Compared to groups I and II, $sPLA_2$ from group III is different except for the conserved active site and the Ca^{2+}-binding loop. The first member of group III was bee venom $sPLA_2$. Its polypeptide chain, containing 135 residues stabilized by five disulfide bridges, showed a three-dimensional structure with three α-helices and a wing-like structure [2].

$sPLA_2$s from scorpion venom belonging to group III that are monomeric are heterodimeric enzymes. They are made up of a long enzymatic chain connected to a short chain by a disulfide bridge following the pentapeptide cleavage throughout the maturation phases. The long chain contains a Ca^{2+}-binding loop and a catalytic dyad [2]. Structural studies of scorpion-venom $sPLA_2$ have been carried out using the only available bee venom $sPLA_2$ crystal structure, showing a significant sequence homology [5]. In all built models, the long enzymatic chain steadied by four disulfide bonds shows three α-helices while the short one is arranged on an antiparallel β-sheet. The long chain is responsible for the phospholipase activity by containing the active site residues and Ca^{2+}-binding loop. Built models suggest that the free cysteine in the short chain is susceptible to establishing an SS bond with the last free cysteine residue in the long chain even when the pentapeptide is excised. The primary structure of the short chain differs between scorpion $sPLA_2$ venom and shows many hydrophobic residues [2,5]. The short chain's role in $sPLA_2$ activity and stability, as well as the influence of the pentapeptide insert, were investigated with only two recombinant forms of Sm-PLGV, a secreted PLA_2 from *Scorpio maurus* venom glands. These two recombinant forms are $rPLA_2$(+5) (formed by the long chain, the pentapeptide, and the short chain) and rPLA(−5) containing long and short chains without the pentapeptide deleted by mutagenesis [5].

The catalytic mechanism of group III $sPLA_2$ is due to the interactions between Asp, His, and tyrosine (Tyr) amino acid residues in the active site [6]. In the well-characterized bee-venom $sPLA_2$, it has been proposed that the His–Asp pair is critical for phospholipid (PL) hydrolysis by PLA_2. Indeed, His-34 acts as a bronstead base and forms hydrogen bonds with the carboxyl and hydroxyl groups of Asp-64 and Tyr-87, respectively [7]. Interestingly, the active site of $MtsPLA_2$ and Sm-PLGV from *Mesobuthus tamulus* and *Scorpio maurus*, respectively, showed that the Asp-62 is substituted by the acidic residue glutamic acid (Glu) [5,6]. Active site analysis of the built $MtsPLA_2$ model revealed that the carboxyl oxygen of the Glu residue is oriented away from the catalytic His residue, preventing the formation of hydrogen bonds between these two residues. The Glu side chain conformation is not conducive to a possible interaction of water with the catalytic His. In its current orientation, the Glu residue is stabilized by interactions with the surrounding residues [6].

In a previous study, infrared spectroscopy analyses, assisted with 3D modeling of the recombinant form of Sm-PLGV designed with $rPLA_2$(−5), were performed, in order to investigate the structure–function relationships. This study underlined the importance of the Tyr residue at position 122 in active site stabilization through interaction with the Glu-63 residue. Indeed, this recombinant enzyme showed a high specific activity of 1500 U/mg with a catalytic efficiency k_{cat}/K_m of 83.6 $s^{-1}{\cdot}mM^{-1}$ compared to the recombinant forms $rPLA_2$(+5) in which lysine residue 124 blocks the interaction of Tyr-122 with Glu-63, allowing a reduction of the specific activity to 500 U/mg [5].

To evaluate the importance of active site residues Glu and Tyr in catalysis, we investigated the kinetic behavior of three different mutants of $rPLA_2$(−5): The residue Glu-63 was substituted by an Asp residue in the first mutant (E63D) and the Tyr-122 residue was replaced by an Arg residue in the second mutant (Y122R). Kinetic behavior was also studied

by constructing the double mutant (D63–R122) and comparing it to the wild-type form ($rPLA_2(-5)$).

2. Materials and Methods

2.1. Materials

Phospholipase substrates (egg phosphatidylcholine (egg-PC), 1,2-dilauroyl-sn-glycero-3-phosphocholine (diC12-PC), and 1,2-dilauroyl-sn-glycero-3-phosphoethanolamine (diC12-PE)), Triton X100, ethylenediaminetetraacetic acid (EDTA), sodium taurodeoxycholate (NaTDC), Bovine Serum Albumin (BSA), β-cyclodextrin, NaCl, isopropyl-thio-β-D-galactopyranoside (IPTG), $CaCl_2$, and Tris–HCl were obtained from Sigma Aldrich (St. Quentin-Fallavier, France). Ammonium persulfate, Coomassie brilliant blue R-250, guanidine hydrochloride; N,N,N′,N′-tetramethyl ethylenediamine (TEMED) acrylamide, Sodium Dodecyl Sulfate (SDS), β-mercaptoethanol, L-cysteine, p-bromophenacyl bromide (p-BPB), and the chromatography column (HisLinkTM Protein Purification Resin) were obtained from Bio-Rad. Restriction endonuclease enzymes were used according to the manufacturer's protocols, and Kanamycin was obtained from Promega (France, Charbonnières-les-Bains).

2.2. Bacterial Strains, Plasmids, and Media

E. coli strains XL1Blue and BL21(DE3) served as cloning and overexpression hosts of $rPLA_2(-5)$ mutants. Transformed *E. coli* strains were grown on LB medium with kanamycin (100 $\mu g \cdot mL^{-1}$). The expression vector was the plasmid pET28b(+). The Wizard polymerase chain reaction (PCR) Preps DNA purification system (Promega) allowed the purification of PCR products.

2.3. Site-Directed Mutagenesis Construction

cDNA encoding $rPLA_2(-5)$ (372 pb) cloned into the pET21a(+) expression plasmid served as the PCR template [6]. The three site-directed mutants E63D, Y122R, and D63–R122 were constructed using the following protocol presented in Table 1. Mutations were made by overlap extension PCR mutagenesis. Selected mutants were verified by DNA sequencing.

PCR reactions were performed in 50 µL reaction mixtures including 0.5 µg of the cDNA template, 1 µmol of each primer, 10 mM dNTP mix, and 1.25 U of DNA polymerase with 10× DNA polymerase buffer. The performed PCR program consisted of three steps: denaturation (1 min at 95 °C), annealing (1 min at 57 °C), and extension (1 min at 72 °C) for 35 cycles. Amplified genes corresponding to mutants E63D, Y122R, and D63–R122 were cloned directionally using *NdeI* and *XhoI* restriction sites in the pET28b(+) expression vector. Plasmid pET28b(+) and mutants were double-digested and purified. Then, the ligation reaction was carried out in the ratio of 3 inserts/1 vector. Selection of *E. coli* BL21(DE3) transformants was performed in LB medium with kanamycin (100 $\mu g \cdot mL^{-1}$). Restriction analysis and DNA sequences were determined in order to verify the presence of appropriate inserts.

Table 1. PCR reactions and primers used to generate $rPLA_2(-5)$ mutants E63D, Y122R, and D63–R122.

Mutant	Primers Used for PCR	cDNA Template	Amplified Region
E63D	PCR 1: Fw: primer 1 Rv: primer 2	The cDNA encoding the $rPLA_2(-5)$ gene formed by 372 pb cloned into the pET21a(+) expression vector.	PCR1 product: 195 bp corresponding to residues 1 to 65 in the protein $rPLA_2(-5)$ sequence.
	PCR 2: Fw: primer 3 Rv: primer 4		PCR2 product: 177 pb encoding the $rPLA_2(-5)$ protein region from residues 66 to 124.
	PCR 3: Fw: primer 1 Rv: primer 4	Amplified products obtained from PCR1 and PCR2.	A cDNA encoding the mutant E63D constructed of 372 pb.

Table 1. *Cont.*

Mutant	Primers Used for PCR	cDNA Template	Amplified Region
Y122R	Fw: primer 1 Rv: primer 5	The cDNA encoding to rPLA$_2$(−5) gene formed by 372 pb cloned into the pET21a(+) expression vector.	A cDNA encoding the mutant Y122R constructed of 372 pb.
D63–R122	Fw: primer 1 Rv: primer 5	A cDNA encoding the mutant E63D constructed of 372 pb.	A cDNA encoding the mutant D63–R122 constructed of 372 pb.

Primer sequences are as follows: **Primer 1**: $^{5'}$GGAATTC**CATATG**TTTCTTATATGGGGAGGGACC$^{3'}$; **Primer 2:** $^{5'}$AGCTTC**G**TCGCATTTGCAGTT$^{3'}$; **Primer 3**: $^{5'}$TTCGATCAGTGCTTGACGGAA$^{3'}$; **Primer 4**: $^{5'}$CCG**CTCGAG**CTAGTCTTTGTAGCTCTTTTTCC$^{3'}$; and **Primer 5**: $^{5'}$CCG**CTCGAG**CTA GTC TTT**CCT**GCTCTTTTTCCA$^{3'}$. Restriction sites of endonucleases *NdeI* and *XhoI* were underlined. The *NdeI* (CATATG) and *XhoI* (CTCGAG) restriction sites were introduced at primers 1, 4, and 5, respectively. The nucleotide modified to generate mutations was marked in red and double-underlined in primers 2 and 5. In primer 2, the codon $^{5'}$TTC$^{3'}$ encoding residue E was replaced by the codon $^{5'}$GTC$^{3'}$ encoding residue D. In primer 5, the codon $^{5'}$GTA$^{3'}$ encoding residue Y was replaced by $^{5'}$CCT$^{3'}$ encoding residue R.

2.4. Expression and Purification

Transformed bacteria BL21(DE3) were grown at 37 °C on LB medium supplemented with kanamycin (100 μg·mL^{-1}) until an absorbance of about 0.6 to 0.8 was observed at 600 nm. Then, 1 mM IPTG was added to induce the expression of recombinant proteins for 5 h. After centrifugation at 4 °C for 15 min at 12,000× *g*, recombinant proteins present in inclusion bodies were first renatured and then purified according to Krayem et al.'s [5] protocol with slight modifications.

The obtained pellet was solubilized in buffer R (50 mM Tris–HCl pH 8.0, including 1 mM EDTA, 0.5 mM PMSF, and 50 mM NaCl) allowing a 20% (*w*/*v*) cell suspension to be obtained. This percentage allowed a maximal yield of well-refolded proteins to be obtained. In order to solubilize inclusion bodies, increasing concentrations (0.4%, 0.8%, and 1% (*w*/*v*)) of sodium deoxycholate (NaDC) and Triton X-100 were added. After stirring for 20 min at 4 °C, sonication using an MSE Sonyprep 150 (Bio-Rad (Hercules, CA, USA) at full power was applied in order to disrupt the cells. After centrifugation at 4 °C (10 min at 15,000× *g*), NaDC and Triton X-100 were eliminated by washing the resulting solid pellet with buffer R. Lastly, inclusion bodies in the pellet were dissolved in 25 mL of buffer R with 5% β-mercaptoethanol and 6 M guanidine hydrochloride under overnight stirring at 4 °C. About 0.8 mg/mL of solubilized denatured recombinant proteins were collected after centrifugation for 10 min at 15,000× *g* and 4 °C.

Protein refolding was carried out according to the protocol previously described [5]. Briefly, obtained denatured recombinant PLA$_2$s were dialyzed 4 times at 4 °C for 48 h against 2 L of 20 mM Tris–HCl at pH 8, including 0.6 M guanidine hydrochloride, 5 mM L-cysteine, and 5 mM $CaCl_2$ (buffer A). Unfolded precipitate proteins were discarded by centrifugation for 10 min at 15,000× *g* and 4 °C, while guanidine hydrochloride, the denatured agent, was removed by dialysis at 4 °C overnight against 2 L of 20 mM Tris–HCl at pH 8, containing 5 mM $CaCl_2$ and 20 mM NaCl (buffer B). The obtained folded protein solution was loaded on the HisLink™ Protein Purification Resin column pre-equilibrated with buffer B. A linear gradient of imidazole (from 20 mM to 400 mM) was then applied to elute proteins after washing the column with buffer B until the optical density at 280 nm dropped to zero. The different recombinant mutants were eluted between 50 mM and 200 mM imidazole. Collected fractions of 1.5 mL were analyzed by measuring the phospholipase activity under standard conditions [5]. Active fractions displaying a unique band in SDS-PAGE were collected and concentrated. The protein content of pure enzymes was measured by following the Bradford protocol [8].

2.5. Phospholipase A_2 Assay

Measurement of PLA_2 activity was performed titrimetrically using a pH-stat technique under standard conditions: The egg phosphatidylcholine (egg-PC) 1% w/v was used as an emulsified substrate with 8 mM NaTDC and 12 mM $CaCl_2$ at pH 8.5 and 50 °C [5]. According to this technique, the release of one μmole of free fatty acids (FFAs) per minute corresponds to one phospholipase A_2 unit.

2.6. Hydrolysis of Phospholipid Monolayers

The interfacial behavior of mutants was assessed using a baro-stat system (KSV-2200 baro-stat (KSV Helsinki)) as previously reported by Pattus et al. [9], using zero-order Teflon, composed of two compartments, and equipped with a mobile Teflon barrier. The latter allows the compensation of substrate molecules removed from the film after enzymatic hydrolysis, thereby keeping a constant surface pressure. Surface pressure was determined using a Wilhelmy plate (perimeter 3.94 cm) attached to an electro-balance, which was sequentially connected to a microprocessor allowing mobile barrier movements to be controlled.

The reaction compartment (120 cm^2) sub-phase (10 mM Tris–HCl pH 8, 20 mM $CaCl_2$, 150 mM NaCl, 0.5 mM β-cyclodextrin, 1 mM EDTA) was continuously stirred at 250 rpm. The reservoir compartment was 249 mm long and 148 mm wide. In order to inject enzyme solution through the film over the stirrer, a Hamilton syringe was used. Hydrolysis of PL monolayers by injecting phospholipases releases water-soluble lyso-PL and FFAs that rapidly desorb from the monolayer. The consequent decreased surface pressure therefore allowed the mobile barrier displacement to maintain a constant surface pressure. As the studied PL monolayers exhibited compression isotherms at the air–water interface, the barrier-covered surface was, consequently, converted into substrate molecules. Phospholipase activity was expressed as the amount of substrate hydrolyzed (moles) per surface and time units of the "zero-order" trough's reaction compartment for an appropriate concentration of $sPLA_2$.

2.7. Hemolysis Assay

The hemolytic activity of the pure mutants E63D, Y122R, and D63–R122 and the wild-type $rPLA_2(-5)$ proteins was investigated against human red blood cells (RBCs) [5]. A pure RBC suspension was obtained from freshly collected anticoagulated blood samples. An amount of 20 mL of phosphate-buffered saline (PBS, pH 7.5) was mixed with 1 mL of blood and centrifuged for 5 min at 4 °C and at 1900× g. Gentle aspiration of the buffy coats and the supernatant was performed to wash the RBCs in the pellet. This process was repeated three times. One milliliter of pure RBC suspension was obtained and used for the hemolytic assay. Various purified phospholipases at a concentration of 400 μg/mL were added to the RBC suspension. After mixing and incubating for 30 min at 37 °C, centrifugation for 5 min at 4 °C and 1500× g was performed. In order to determine the extent of RBC lysis and hemoglobin liberation, the absorbance of supernatants was recorded at 545 nm. RBCs in PBS alone or with 1% Triton X-100 served as a negative control (0% hemolysis) or positive control (100% hemolysis), respectively.

2.8. Temperature and pH Stability

The thermal stability of the three mutants of $rPLA_2(-5)$ was studied by incubating aliquots of corresponding enzymes for 1 h at different temperatures ranging from 25 °C to 85 °C. Residual activities were measured after centrifugation for 5 min at 13,000× g and 4 °C under the standard assay method [5]. pH stability was also checked by incubating the different recombinant mutants for 1h in the following buffers: sodium acetate buffer (50 mM, pH 4–6), potassium phosphate buffer (50 mM, pH 6–8), Tris–HCl buffer (50 mM, pH 7–9), and glycine–NaOH buffer (50 mM, pH 10–12). Residual activities were measured after centrifugation for 5 min at 13,000× g and 4 °C under the standard assay method [5].

2.9. Molecular Modeling

The construction of 3D models of phospholipases was performed by the automated comparative protein structure homology modeling server, SWISS-MODEL (http://www.expasy.org/swissmod, accessed on 1 November 2023), using the crystal structure complex of bee venom PLA_2 (PDB code: 1POC) as a template.

Exploration of molecular interactions between catalytic residues and those around the active site was carried out using the discovery studio visualizer (DSV) and Viewer Lite.

3. Results

3.1. Protein Expression and Purification

Recombinant mutants E63D, Y122R, and D63–R122 were obtained after refolding and purification following the protocol described in Section 2 (Figure 1A).

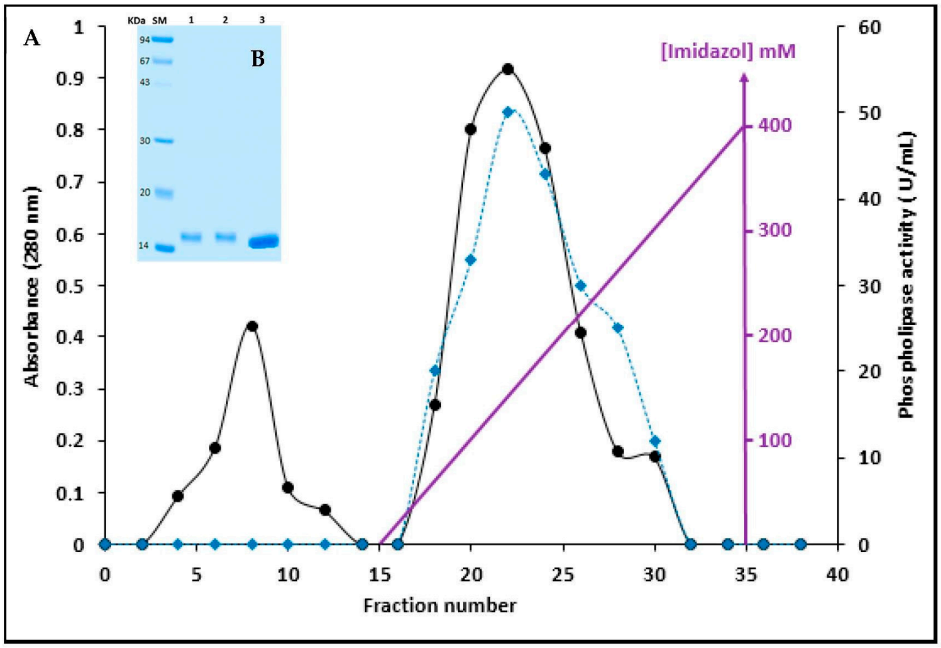

Figure 1. Chromatography profile of $rPLA_2(-5)$ mutants on affinity chromatography column and electrophoresis analysis. (**A**) Phospholipase activity (blue line), absorbance at 280 nm (dark line). The HisLink^{TM} Protein Purification Resin column was pre-equilibrated with buffer B. After washing the column with buffer B until no absorbance could be recorded at 280 nm, a linear gradient of imidazole (from 20 mM to 400 mM) was applied to elute recombinant mutants between 50 mM and 200 mM. (**B**) Analysis of purified recombinant E63D, Y122R, and wild $rPLA_2(-5)$ by SDS-PAGE (15%). SM: size marker, Lane 1: E63D; Lane 2: Y122R; Lane 3: wild $rPLA_2(-5)$.

PLA_2 activity was investigated on egg-PC as an emulsified substrate by the pH-stat method according to the same conditions used for wild $rPLA_2(-5)$ (in the presence of 8 mM NaTDC and 12 mM $CaCl_2$ at pH 8.5 and 50 °C) [5]. While the double mutant D63–R122 did not exhibit any enzymatic activity, E63D and Y122R displayed PLA_2 activities of about 3 ± 1 and 14 ± 2 U/mL, respectively (Table 2). Under the same conditions, the wild-type $rPLA_2(-5)$, however, showed an enzymatic activity of about 750 U/mL. Specific activities on the emulsified substrate PC were 1500 U/mg, 35 U/mg, and 9.3 U/mg for wild type $rPLA_2(-5)$, E63D, and Y122R, respectively. The double mutant D63–R122 was fully inactive (Table 2). These findings thus revealed the importance of the modified residues on phospholipid hydrolysis.

Table 2. Purification steps and specific activities (SAs) of E63D, Y122R, and D63–R122. Proteins were overexpressed in *E. coli* cells using the pET-28b(+) expression vector and each purification was performed using one liter of culture. Phospholipase activity was measured using emulsified egg-PC as substrate with pH-stat technique. Purified wild rPLA$_2$(−5) was taken as a control for specific activity comparison. Experiments were repeated three times.

Purification Steps	[Proteins] (mg/mL) [a]	Total Proteins (mg)	Activity (U/mL) [b]	Specific Activity (U/mg)	Proteins Recovery (%)
Inclusion bodies solubilization	0.42 ± 0.12	8.5 ± 0.21	-	-	-
E63D					
Refolding	0.32 ± 0.13	6.4 ± 0.19	3 ± 1	9.3 ± 2	75.29 ± 5
Affinity chromatography	0.60 ± 0.21	1.2 ± 0.11	50 ± 4	82.5 ± 4	18.75 ± 4
Y122R					
Refolding	0.30 ± 0.17	6 ± 0.18	14 ± 2	35 ± 3	70.42 ± 8
Affinity chromatography	0.65 ± 0.18	1.5 ± 0.16	70 ± 5	107 ± 6	21.66 ± 3
D63–R122					
Refolding	0.29 ± 0.15	5.8 ± 0.15	0	0	68.23 ± 10
Affinity chromatography	0.71 ± 0.2	1.48 ± 0.2	0	0	24.13 ± 4
rPLA$_2$(−5)					
Refolding	1.25 ± 0.5	6 ± 2	375 ± 15	300 ± 18	70.58 ± 3
Affinity chromatography	0.5 ± 0.25	3 ± 0.5	750 ± 20	1500 ± 27	50 ± 4

[a]: Proteins were estimated by Bradford method [8]. [b]: One unit of phospholipase activity corresponds to the liberation of 1 µmol of FFAs under standard conditions [5].

From 1 L culture, protein recoveries between 68 and 75% were obtained after refolding of the three mutants. A similar recovery of 70.58% was recorded with the wild-type rPLA$_2$(−5) (Table 2). The high recovery might be due to the high amount of aggregate recombinant enzymes produced in *E. coli* cells in inclusion bodies. Indeed, 8 mg of total proteins were obtained for rPLA$_2$(−5) and the three mutants (Table 2). After refolding, about 5 and 6 mg of total refolded proteins were obtained for rPLA$_2$(−5), E63D, Y122R, and D63–R122. Table 2 shows a difference in the yields of pure refolded proteins: about 1.5 mg/mL for the three pure mutants and 3 mg/mL for the pure wild-type rPLA$_2$(−5). This could be attributed to the increased rate of misfolding and protein aggregation in the case of mutants during the dialysis step. E63D, Y122R, and D63–R122 were purified with a final yield between 18 and 24% compared to 50% for the wild-type rPLA$_2$(−5) (Table 2). In the SDS-PAGE analysis, purified mutants showed a single band corresponding to the expected molecular mass around 15 kDa (Figure 1B).

3.2. Apparent Kinetic Parameter Determination

Apparent kinetic parameters such as the Michaelis Menten constant (K_m), catalytic constant (k_{cat}), and the catalytic efficiency (k_{cat}/K_m) of E63D, Y122R, and D63–R122 were determined compared to the wild form rPLA$_2$(−5). Under standard conditions, specific activities of the three mutants were determined as a function of increased concentrations of PC [5]. Apparent K_m, k_{cat}, and k_{cat}/K_m were then deduced from the obtained Lineweaver–Burk plots.

While wild rPLA$_2$(−5) exhibited a V_{max} value of 1500 µmol/min/mg, mutants E63D and Y122R showed a V_{max} reduction of 82.5 ± 4 µmol/min/mg and 107 ± 6 µmol/min/mg, respectively. Compared to the wild rPLA$_2$(−5), which exhibited a K_m value of 4.23 ± 0.35 mM, K_m values of 8.33 ± 2 mM and 1.8 ± 0.7 mM were recorded for E63D and Y122R, respec-

tively. However, mutants had highly reduced k_{cat} values, indicating that they had different numbers of converted substrates into products (Table 3).

Table 3. E63D, Y122R, and D63–R122 apparent kinetic parameters. Wild $rPLA_2(-5)$ overexpressed in *E. coli* was taken as control. Experiments were repeated three times.

Enzymes	V_{max} (μmol/min/mg)	K_m (mM)	k_{cat} (s^{-1})	K_{cat}/K_m ($s^{-1} \cdot mM^{-1}$)	Reference
$rPLA_2(-5)$	1500 ± 7	4.23 ± 0.35	354 ± 2	83.86 ± 8	[5]
E63D	9.3 ± 2	8.33 ± 2	32.7 ± 1.5	3.92 ± 2.3	Present study
Y122R	107 ± 6	1.8 ± 0.7	25.4 ± 3	14.11 ± 2	
D63–R122	0	0	0	-	

These results confirmed our previous structural study in which we constructed a 3D model for the wild $rPLA_2(-5)$ [5]. In this study, we have demonstrated the importance of Glu-63 in the catalytic activity compared to bee venom $sPLA_2$, which has an Asp residue in the same position. FTIR data and 3D modeling of $rPLA_2(-5)$ suggested that the pentapeptide deletion allowed a structural reorganization of the short chain responsible for the formation of a productive Glu-63/His-34 interaction with the Ca^{2+}-binding residues [5]. Similarly, an in silico study of the $MtPLA_2$ from *Mesobuthus tamulus* venom showed that catalytic Glu is stabilized by numerous interactions with the surrounding residues in the Ca^{2+}-binding loop [6]. In the bee-venom $sPLA_2$, in order to analyze the impact of the Asp-64 carboxylate on the enzyme's catalytic function, the substitution of Asp-64 with asparagine caused a moderate decrease in the enzyme's catalytic efficiency (56-fold in k_{cat} and 10-fold in k_{cat}/K_m) [10].

The reduction in Y122R V_{max} can be related to an absence of the interaction of Arg residues with Glu-63 and His-34. Indeed, in our previous structural study, Tyr-122 in the access behind Glu-63 stabilized the interaction between Glu-63 and His-34 residues via a hydrogen bond with Glu-63's phenolic hydroxyl function. Similarly, the catalytic sites of group I and II PLA_2 were found to be stabilized by two Tyr residues [5]. In the well-studied group III bee-venom $sPLA_2$, the substitution of Tyr-87 by a phenylalanine residue resulted in the enzyme's catalytic efficiency being reduced 5-fold when compared to wild $sPLA_2$ [10].

3.3. Molecular Modeling Analysis

In order to explain the observed reduction in the specific activities and kinetic parameters of mutants compared to the wild $rPLA_2(-5)$, 3D models were constructed using the only available group III complex structure of bee-venom PLA_2 as the template (PDB code: 1POC) [11]. Figure 2A showed a superposition of $rPLA_2(-5)$ and bee-venom PLA_2 models and the orientation of Glu-63 and Tyr-122 side-chain residues. Analysis of active site amino acids in $rPLA_2(-5)$ (Figure 2B) revealed that Glu-63 interacted via hydrogenous bonds with Asn-59, Cys-60, Phe-66, and Asp-67 as well as with Glu-64. These active site-stabilizing bindings in each constructed mutant (E63D, Y122R, and D63–R122) allowed the observation of some modifications in the orientation plan of side chain residues and the nature of interactions (Figure 2B–D). Indeed, it seemed that Glu-64 played an important role in the stabilization of catalytic residues since its orientation and interaction were modified in each mutant configuration (Figure 2B–D). The reduction in the specific activity of the mutant E63D could be attributed to the modification of binding with the hydroxyl group of Tyr-122 as well as the orientation of the Glu-64 radical (Figure 2C). The side chain of Arg-122 in the mutant Y122R was oriented away from Glu-63 and Glu-64, with the absence of the characteristic interaction of Glu-63 with Tyr-122 (Figure 2C). Compared to the wild-type and simple mutants E63D and Y122R, the plan orientation of all interactions was different in the double mutant D63–R122 (Figure 2E). Indeed, the Asp-63 side chain did not interact

with Arg-122, which was near the radical residues Cys-60 and Cys-100. Furthermore, the orientation of hydrogen bonds linking the side chains of Asp-63 and Asp-64 and between Asp-63, Asn-59, and Cys-60 were different compared to the simple mutant (Figure 2E). This new interaction network destabilized the substrate binding during hydrolysis. Thus, it could be concluded that the hydrogen-binding network linking Glu-63, Tyr-122, and Glu-64 was critical for catalysis.

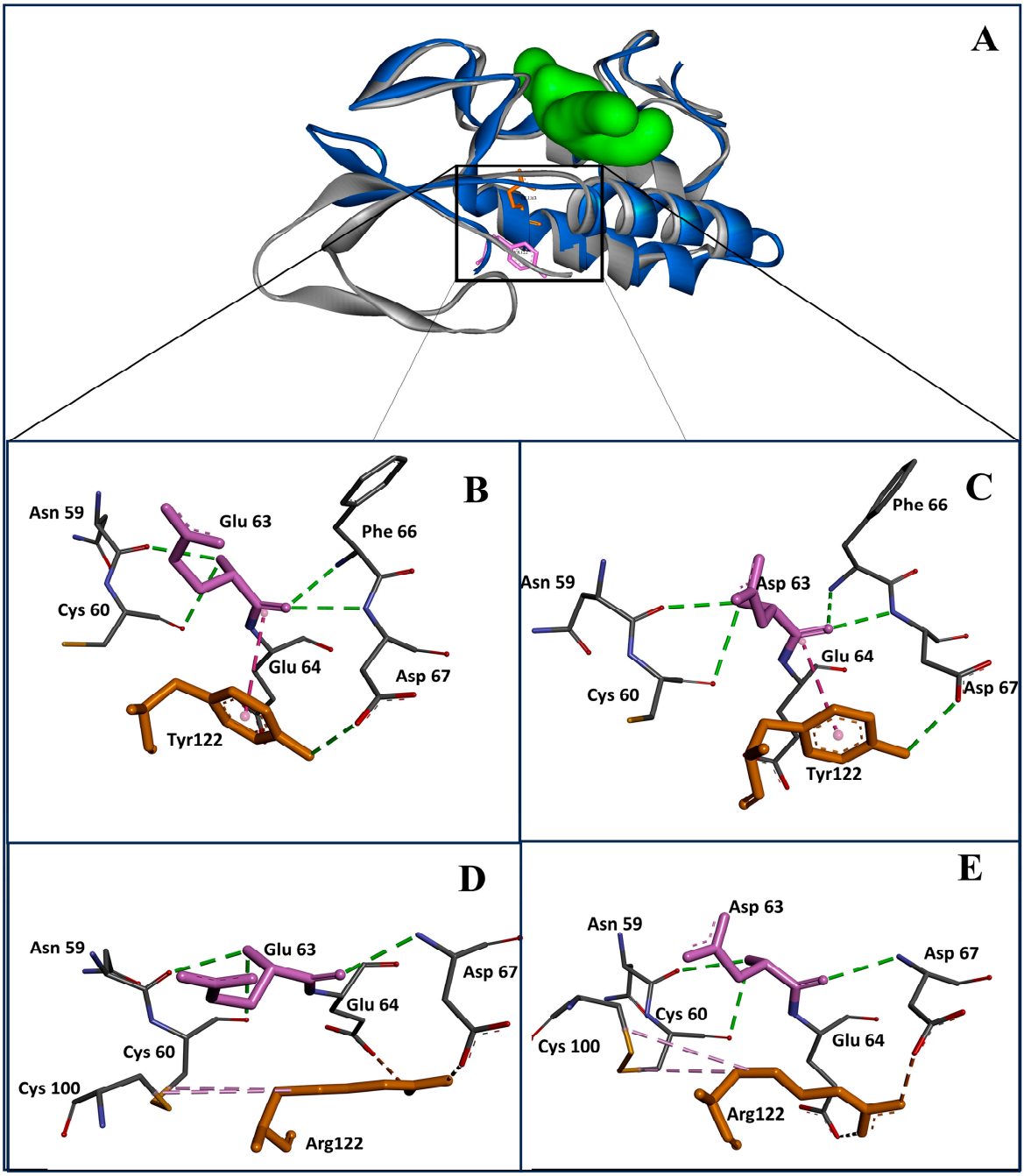

Figure 2. Three-dimensional structural modeling of rPLA$_2$(−5) and the three constructed mutants E63D, Y122R, and D63–R122. (**A**) Superposition of rPLA$_2$(−5) model (grey) and bee-venom PLA$_2$ (PDB code: 1POC) structure (blue) generated by Viewer Lite. (**B**) Residue interactions with Glu-63 in the wild type rPLA$_2$(−5), (**C**) E63D, (**D**) Y122R, and (**E**) the double mutant D63–R122. Glutamate radical is shown in pink and Tyrosine radical is shown in brown. Conventional hydrogen bonds are colored in green and the alkyl bonds are shown in pink.

3.4. Stability Study

The stability of the mutant proteins towards pH and temperature was also investigated in addition to their catalytic activity. The pH stability assessment of E63D, Y122R, and D63–R122 maintained at 50 °C, which corresponds to the optimum temperature of wild rPLA$_2$(−5) activity, was performed [5]. All mutants were incubated in different pH solutions (3–12) and at 4 °C, followed by measuring their residual activities under standard conditions [5].

Maximum protein stability was observed at pH 8 with 83.3% and 100% for rPLA$_2$(−5) and E63D, respectively (Figure 3A). Observed pH stability can be related to the rigid tridimensional conformation of sPLA$_2$ through the highly disulfide-linked tertiary structure (10 SS bonds).

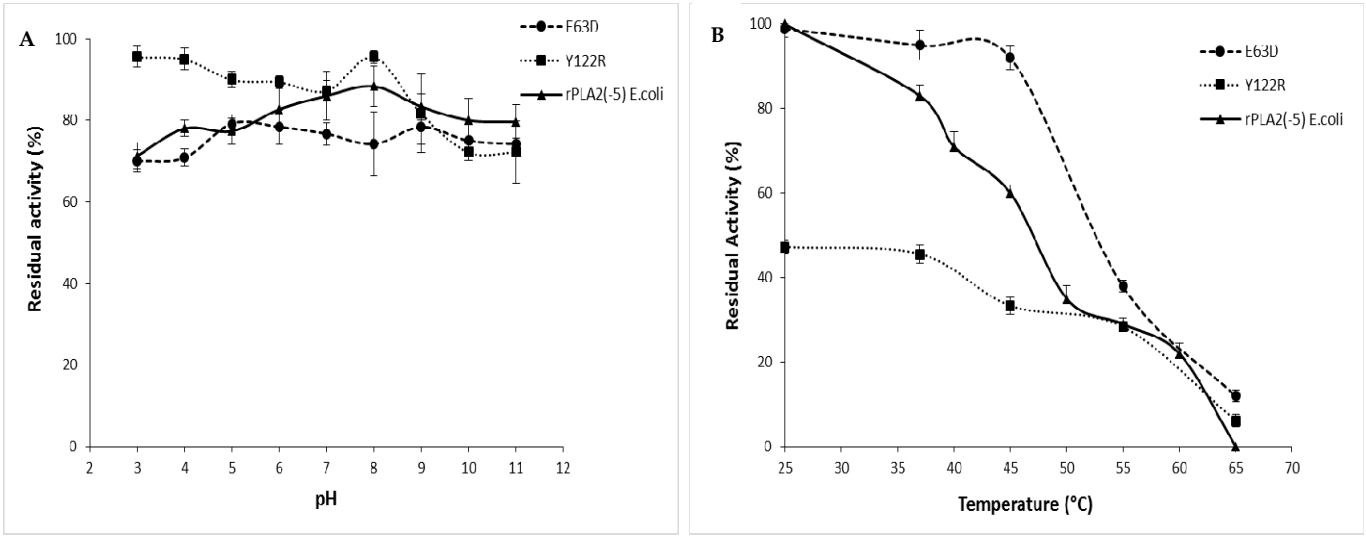

Figure 3. pH and temperature stability of E63D, Y122R, and wild rPLA$_2$(−5). (**A**) pH stability was performed after 30 min incubation of each enzyme in different pH solutions. (**B**) Thermostability of recombinant mutants was tested by measuring their residual activities after 1 h incubation at different temperatures. Experiments were repeated three times.

The thermostability of E63D, Y122R, and D63–R122, compared to wild rPLA$_2$(−5), was studied by measuring the remaining activity after 1 h incubation at different temperatures (25–80 °C) (Figure 3B). Our results showed that E63D exhibited a similar thermostability to wild rPLA$_2$(−5). Decreased enzymatic activity was observed as temperature increased and was totally lost at 65 °C. Y122R was less thermostable and lost more than 50% of its activity at 25 °C (Figure 3B).

3.5. Correlation between Hemolytic Effect and Phospholipase Activity with Surface Pressure

Secreted phospholipases A$_2$, which have a variety of behaviors against biological membranes, have been useful tools to investigate lipid localization in membranes like erythrocytes. These enzymes are characterized by a different ability to penetrate these membranes.

In our previous study, we showed that at 400 µg/mL corresponding to 0.28 µM, rPLA$_2$(−5) exhibited a hemolytic effect on human RBCs evaluated to be 97% of hemolysis. This activity was directly dependent on the catalytic activity since the enzyme inactivated by p-BPB (p-bromophenylacyl bromide) became unable to hydrolyze membrane RBCs [5]. E63D and Y122R with reduced specific activities exhibited 15 and 17% hemolytic effect, respectively, at the same concentration. The inactive double mutant D63–R122 had no effect on RBCs. Our data confirmed the correlation between phospholipase activity and hemolysis as previously reported for other snake venom sPLA$_2$s, such as NK-PLA$_2$-I and NK-PLA$_2$-II isolated from *Naja kaouthia* cobra venom. Indeed, at 500 nM, NK-PLA$_2$-I

and NK-PLA_2-II hydrolyzed PLs in human RBC membranes while enzymes inhibited by 3.3 mM of p-BPB were unable to penetrate these membranes [12].

It is well documented that PLA_2 hemolytic activity was correlated with PL composition and asymmetric organization of human RBC membranes in their inner and outer leaflets. Zwitterionic PE is mostly located in the inner monolayer, whereas sphingomyelin (SM) and PC characterize the outer monolayer [13]. This asymmetric PL organization could explain the different behavior of several $sPLA_2$s on RBC membranes as well as in the PL layer. In this line, in order to investigate the potential association between PL hydrolysis in RBC membranes causing hemolysis and the enzyme's capability to penetrate PL layers at high surface pressure, the activity of E63D, Y122R, as well as the wild $rPLA_2(-5)$ on PL monolayers at several surface pressures, was evaluated. The kinetic behavior on zwitterionic PL monolayers of recombinant E63D and Y122R mutants compared to $rPLA_2(-5)$ was evaluated.

E63D and Y122R showed the same PL preference of wild $rPLA_2(-5)$ and were more active on diC12-PE films than on diC12-PC ones (Figure 4). The maximal enzymatic activities of E63D were reached on diC12-PE at 30 $mN{\cdot}m^{-1}$. A specific activity of about 5.68 $mol{\cdot}cm^{-2}{\cdot}min^{-1}{\cdot}M^{-1}$ was observed for E63D compared to 7.47 $mol{\cdot}cm^{-2}{\cdot}min^{-1}{\cdot}M^{-1}$ for wild $rPLA_2(-5)$ (Figure 4A). Furthermore, in the diC12-PC, SA for E63D and Y122R were 0.27 and 0.03 $mol{\cdot}cm^{-2}{\cdot}min^{-1}{\cdot}M^{-1}$ at 30 $mN{\cdot}m^{-1}$ respectively (Figure 4B).

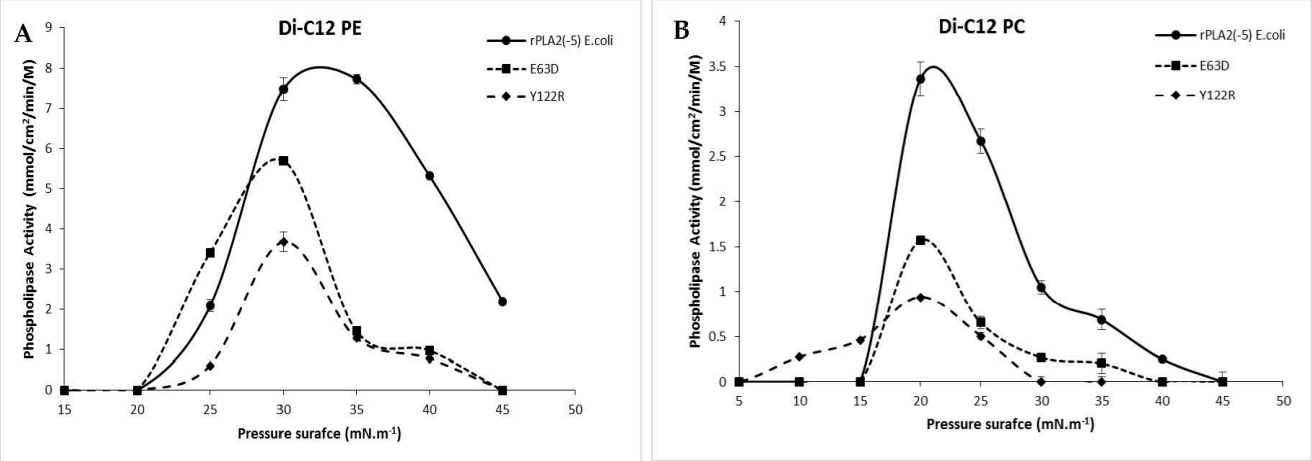

Figure 4. Activities on phospholipid monolayers (diC12-PC (**A**), diC12-PE (**B**)) of wild $rPLA_2(-5)$ and mutants (E63D and Y122R) with increasing surface pressure. Phospholipase activities were expressed as the number of moles of phospholipids hydrolyzed by units of surface and units of time of the "zero-order" reaction compartment. Experiments were repeated three times.

Hydrolysis of diC12-PC monolayers demonstrated the highest specific activities for E63D (1.56 $mol{\cdot}cm^{-2}{\cdot}min^{-1}{\cdot}M^{-1}$) and $rPLA_2(-5)$ (3.63 $mol{\cdot}cm^{-2}{\cdot}min^{-1}{\cdot}M^{-1}$) at 20 $mN.m^{-1}$ (Figure 4B). This reduced SA towards zwitterionic PL monolayers underlines the importance of the modified residue in the catalytic activity shown with the pH-stat system with PL emulsion. A similar finding was observed with the D64E bee PLA_2 mutant, which exhibited lower catalytic activity compared to the wild form but better substrate binding [10].

The difference observed in the hydrolysis of zwitterionic PL monolayers PC and PE could be related to the difference in interfacial binding to these PLs depending on their physical state and polar head. Interfacial binding of $sPLA_2$ is mediated by the interaction between the interface-binding surface of the enzyme, around the hydrophobic pocket leading to the active site, and the PL interface film [5].

4. Conclusions

In all secreted phospholipases A_2, Asp-62 is the key residue in the active site that interacts with Tyr-87. However, scorpion-venom heterodimeric $sPLA_2$ showed the implications of Glu-63 and Tyr-122 in the active site stability. Modification of these residues caused a reduction in specific activity and apparent kinetic parameters. Furthermore, the simple mutants E63D and Y122R remained stable in acidic and alkali pH, whereas the double mutant D63–R122 was catalytically inactive. Mutants' kinetic behaviors on monolayers of zwitterionic PLs at high surface pressure were similar to those of the wild-type form with slightly modified specific activities. This reduction in specific activity could be related to the modification of the interactions of residues around the active site, as shown in the in silico study. To our knowledge, this is the first study that investigated the structure–function relationships of scorpion-venom PLA_2. These mutants might serve as a starting point for pursuing the study of the antitumor effect of scorpion-venom PLA_2, which was previously demonstrated to be independent of the enzymatic activity.

Author Contributions: All authors contributed to the study's conception and design. Material preparation, data collection, and analysis were performed by N.K., M.A., B.K., S.C., A.K., H.H. and A.B.B. The first draft of the manuscript was written by N.K. and A.B.B. All authors have read and agreed to the published version of the manuscript.

Funding: This research received no external funding.

Data Availability Statement: The data presented in this study are available on request from the corresponding author.

Acknowledgments: The authors extend their appreciation to the Deputyship for Research and Innovation, "Ministry of Education", in Saudi Arabia for funding this research (IFKSUOR3-230-4).

Conflicts of Interest: The authors declare no conflict of interest.

References

1. Ivanušec, A.; Šribar, J.; Križaj, I. Secreted phospholipases A_2—Not just enzymes: Revisited. *Int. J. Biol. Sci.* **2022**, *18*, 873. [CrossRef] [PubMed]
2. Krayem, N.; Gargouri, Y. *Scorpion venom* phospholipases A_2: A minireview. *Toxicon Off. J. Int. Soc. Toxinol.* **2020**, *184*, 48–54. [CrossRef] [PubMed]
3. Suranse, V.; Jackson, T.N.; Sunagar, K. Contextual constraints: Dynamic evolution of snake venom phospholipase A_2. *Toxins* **2022**, *14*, 420. [CrossRef]
4. Soltan-Alinejad, P.; Alipour, H.; Meharabani, D.; Azizi, K. Therapeutic potential of bee and scorpion venom phospholipase A_2 (PLA_2): A narrative review. *Iran. J. Med. Sci.* **2022**, *47*, 300.
5. Krayem, N.; Parsiegla, G.; Gaussier, H.; Louati, H.; Jallouli, R.; Mansuelle, P.; Carrière, F.; Gargouri, Y. Functional characterization and FTIR-based 3D modeling of full length and truncated forms of *Scorpio maurus* venom phospholipase A_2. *Biochim. Biophys. Acta (BBA)-Gen. Subj.* **2018**, *1862*, 1247–1261. [CrossRef] [PubMed]
6. Hariprasad, G.; Kumar, M.; Srinivasan, A.; Kaur, P.; Singh, T.P.; Jithesh, O. Structural analysis of a group III Glu62-phospholipase A_2 from the scorpion, *Mesobuthus tamulus*: Targeting and reversible inhibition by native peptides. *Int. J. Biol. Macromol.* **2011**, *48*, 423–431. [CrossRef] [PubMed]
7. Castro-Amorim, J.; Novo de Oliveira, A.; Da Silva, S.L.; Soares, A.M.; Mukherjee, A.K.; Ramos, M.J.; Fernandes, P.A. Catalytically Active Snake Venom PLA_2 Enzymes: An Overview of Its Elusive Mechanisms of Reaction: Miniperspective. *J. Med. Chem.* **2023**, *66*, 5364–5376. [CrossRef] [PubMed]
8. Bradford, M.M. A rapid and sensitive method for the quantitation of microgram quantities of protein utilizing the principle of protein-dye binding. *Anal. Biochem.* **1976**, *72*, 248–254. [CrossRef] [PubMed]
9. Pattus, F.; Slotboom, A.J.; de Haas, G.H. Regulation of the interaction of pancreatic phospholipase A_2 with lipid-water interfaces by Ca^{2+} ions: A monolayer study. *Biochemistry* **1979**, *18*, 2698–2702. [CrossRef] [PubMed]
10. Annand, R.R.; Kontoyianni, M.; Penzotti, J.E.; Dudler, T.; Lybrand, T.P.; Gelb, M.H. Active site of bee venom phospholipase A_2: The role of histidine-34, aspartate-64 and tyrosine-87. *Biochemistry* **1996**, *35*, 4591–4601. [CrossRef] [PubMed]
11. Scott, D.L.; Otwinowski, Z.; Gelb, M.H.; Sigler, P.B. Crystal structure of bee-venom phospholipase A_2 in a complex with a transition-state analogue. *Science* **1990**, *250*, 1563–1566. [CrossRef] [PubMed]

12. Doley, R.; King, G.F.; Mukherjee, A.K. Differential hydrolysis of erythrocyte and mitochondrial membrane phospholipids by two phospholipase A_2 isoenzymes (NK-PLA2-I and NK-PLA2-II) from the venom of the Indian monocled cobra *Naja kaouthia*. *Arch. Biochem. Biophys.* **2004**, *425*, 1–13. [CrossRef] [PubMed]
13. Devaux, P.F. Static and dynamic lipid asymmetry in cell membranes. *Biochemistry* **1991**, *30*, 1163–1173. [CrossRef] [PubMed]